Journal of Heat and Mass Transfer Research

Journal homepage: https://jhmtr.semnan.ac.ir

Semnan University

Research Article

Spectral Quasi-Linearization Approach for Unsteady MHD Boundary Layer Flow of Casson Fluid Due to an Impulsively Stretching Surface

Adeyemi Isaiah Fagbade *

[a]*Department of Mathematical Sciences, Federal University of Technology,P.M.B 704,Akure Ondo State, Nigeria.*

PAPER INFO

Paper history:

Received: 2015-05-03
Revised: 2015-09-20
Accepted: 2016-06-20

Keywords:

Casson fluid;
Magnetohydrodynamic flow;
Magnetic field;
Boundary layer;
Spectra quasi-linearization method;
Impulsively stretching sheet;
Separated by semicolons.

ABSTRACT

The present paper seeks to examine a numerical method of solution called spectra quasi-linearization method (SQLM) to the problem of unsteady MHD boundary layer flow of Casson fluid due to an impulsively stretching surface under the influence of a transverse magnetic field, which is an important physical phenomena in engineering applications. The study extends the previous models to account for a classical non-newtonian fluid called Casson fluid under the influence of a transverse magnetic field. The flow model is described in terms of a highly nonlinear partial differential equations. The method of solution Spectral quasi-linearization methods(SQLM) seeks to linearised the original system of PDEs using the Newton-Raphson based quasilinearization method (QLM). The numerical results for the surface shear stress are compared with those of the analytical approach results, and they are found to be in good agreement. The flow controlling parameters are found to have a profound effect on the resulting flow profiles. It is observed that there is a smooth transition from the small time solution to the large time solution. The magnetic field significantly affects the flow field and skin friction coefficient. Indeed, skin friction coefficient is found to decrease rapidly, initially, in small time interval before attaining a steady state for large time.

DOI: 10.22075/jhmtr.2016.422

1. Introduction

The problem of unsteady convective mass and heat transfer has long been a major subject in the heat transfer theory because of its great importance from both a theoretical and practical viewpoint. In fact there is no actual flow situation, natural or artificial, which does not involve some unsteadiness and examples of unsteady convective flows are very numerous (see [1]). These flows are frequently encountered in technological and environmental situations, such as, energy conservation processes, buildings and structures, the processing of materials, geophysical and biological flows, and the spread of pollutants and fires as well as many others. In the broad class of fluid and heat transfer problems there are two main categories of truly unsteady problems, namely linear and nonlinear problems. However, most viscous flow problems fall into the second class, which are, of course, more difficult to analyze and model. On the other hand, since most of the fundamental concepts which can be described by linear theory are now fairly well understood, the greatest challenges today are in nonlinear situations. Hence, our attention in this paper is focused on unsteady nonlinear MHD convective boundary layer flow problem of Casson fluid over an impulsively stretching surface. The flow and heat transfer problem in the boundary-layer induced by a continuously moving or stretching surface is important in many manufacturing processes. In industry for

* *Corresponding Author: Adeyemi Isaiah Fagbade.*
Email: yemi2favours@yahoo.co.uk

instance, polymer sheets and filaments are manufactured by continuous extrusion of the polymer from a die to a wind up roller which is located at finite distant way Chiam [2]. During many mechanical forming processes, such as extrusion, melt-spinning, etc., the extruded material issues through a slot or die. The ambient fluid condition is stagnant but a fluid flow is induced close to the material being extruded, due to the moving surface. In regions away from the slot or die the fluid flow may be considered to be of a boundary-layer type, although this is not true in the vicinity of the slot or die. Similar situations prevail during the manufacture of plastic and rubber sheets where it is often necessary to blow a gaseous medium through the material which is not, as yet, solid, and where the stretching force may be varying with time (see [3]).

Another typical example of industrial application that belongs to the class of boundary-layer flow problems due to moving surfaces is the cooling of a large metallic plate in a bath, which may be an electrolyte. In this case the fluid flow is induced due to the shrinking of the plate [4]. Glass blowing, continuous casting and the spinning of fibres also involve the flow due to a stretching surface. The first study on the boundary-layer adjacent to a continuous moving surface was conducted by Sakiadis [5] and since then it has been much generalized and refined. The fluid flow problem due to a continuously moving surface in an ambient fluid differs from that of the fluid flow past a fixed surface. Unlike the flow past a fixed surface, the continuous moving surface sucks the ambient fluid and pumps it again in the downstream direction. However, in all the earlier studies on boundary-layer flows due to a moving surface , the effects of the transverse magnetic field was neglected. Liao [6] investigated an analytical solution of unsteady boundary-layer flows caused by an impulsively stretching plate. Roslindar et al. [7] studies unsteady boundary layer flow due to am impulsively stretching surface. In their paper, the stretching velocity is assumed to vary linearly with the distance along the sheet and solved numerically using keller-box method. They observed a smooth transition from the small time solution to the large- time solution. Takhar et al. [8] also studied unsteady three-dimensional MHD-boundary layer flow due to the impulsive motion of a stretching surface. Hayat et al. [9] investigated the influence of soret and dufour effect on magnetohydrodynamics MHD flow of casson fluid. In the above mentioned literatures, the fluid viscosity and thermal conductivity were assumed to be constant value within the boundary layer. Prasad and Vajravelu [10] investigated the effect of variable thermal conductivity in a non-isothermal sheet stretching through power law fluids. Abel et al. [11] examined the combined effects of thermal buoyancy and variable thermal conductivity on a magnetohydrodynamic flow and the associated heat transfer in a power-law fluid past a vertical stretching sheet in the presence of a nonuniform heat source and observed that variable thermal conductivity parameter increases the wall shear stress in the boundary layer region. Bhattacharyya and Pop [12] reported the influence of external magnetic field on the Casson flow over an exponentially shrinking sheet. Recently, Bhattacharyya studied boundary layer stagnation point of Casson fluid and heat transfer towards a shrinking/stretching sheet. It is established that the thermo-physical properties of fluid play a significant role in the engineering applications as seen in aerodynamics, geothermal systems, crude oil extraction,ground water pollution, thermal insulation, heat exchanger, storage of nuclear waste etc.

It is well known that most fluids which are encountered in chemical and allied processing applications do not adhere to the classical Newtonian viscosity postulate and are accordingly known as non-Newtonian fluids Astarita and Marrucci [14]. One particular class of materials which are of considerable practical importance is that in which the viscosity depends on the shear stress or on the flow rate. Most slurries, suspensions and dispersions, polymer solutions, melts and solutions of naturally occurring high-molecular-weight, synthetic polymers, pharmaceutical formulations, cosmetics and toiletries, paints, biological fluids, synthetic lubricants and foodstuffs, exhibit complex rheological behaviour which is not experienced when handling ordinary low-molecular-weight Newtonian fluids such as air, water, silicon oils, etc. Due to the importance of the applications of non-Newtonian fluids for the design of equipment and in industrial processing, considerable efforts have been directed towards the analysis and understanding of such fluids. Further, a fairly large body of fundamental research on non-Newtonian fluid flow can also be found in a number of excellent review articles [15],[16]. A classical example of non-newtonian fluid is Casson fluid. Casson fluid is one of the types of such non-Newtonian fluids, which behaves like an elastic solid such that a yield shear stress exists in the constitutive equation. Some materials e.g. muds, condensed milk,emulsions,paints, printing ink,sugar solutions, exhibit almost all the properties of non-Newtonian fluid. This rheological model was introduced originally by Casson [17] in his research on a flow equation for pigment oil-suspensions of printing ink. Casson model constitutes a plastic fluid model which exhibits shear thinning characteristics, yield stress, and high shear viscosity. According to a research reported by Rao et al. [18], it is stated that Casson fluid model is reduced to a Newtonian fluid at a very high wall shear stress, i.e., when the wall stress is much greater than yield stress. This fluid model also approximates reasonably well the rheological behavior of other liquids including physiological suspensions, foams, cosmetics, syrups, etc. Although different

models are proposed to explain the behavior of non-Newtonian fluids, the most important non-Newtonian fluid possessing a yield value is the Casson fluid. Bird et al. [19] investigated the rheology and flow of visco-plastic materials and reported that the Casson model constitutes a plastic fluid model which exhibits shear thinning characteristics, yield stress, and high shear viscosity. The fundamental analysis of the flow field of non-Newtonian fluids in a boundary layer adjacent to a stretching sheet or an extended surface is very important and is an essential part in the study of fluid dynamics and heat transfer in Mukhopadhyay [20]. The unsteady boundary layer flow and heat transfer of a Casson fluid over a moving flat plate with a parallel free stream were studied by Mustafa et al. [21] and they solved the problem analytically using the Homotopy analysis method (HAM).

The effects of transverse magnetic field on a boundary layer control and on the performance of many systems using electrically conducting fluid such as MHD power generators, cooling of nuclear reactors, plasma studies, etc. has been widely investigated and reported in literatures. Magneto-hydrodynamics (MHD) as a branch of fluid mechanics deals with the study of electrically conducting fluids and electromagnetic forces Srinivasa and Eswara [22]. The idea of MHD is that magnetic fields induce currents in a moving conductive fluid, which create forces on the fluids, and also change the magnetic field itself. MHD problems arise in a wide variety of situations ranging from the explanation of the origin of Earth's magnetic field and the prediction of space weather to the damping of turbulent fluctuations in semiconductor melts during crystal growth and, even in the measurement of the flow rates of beverages in food industry. An interesting application of MHD to metallurgy lies in the purification of molten metals from non-metallic inclusions by the application of a transverse magnetic field. In recent years, MHD flow problems have become more important industrially. Indeed, MHD laminar boundary layer behavior over a stretching surface is a significant type of flow having considerable practical applications in chemical engineering, electrochemistry and polymer processing. The laminar boundary layer on a moving continuous flat surface in the presence of suction and magnetic field was studied by Shrivastava [23]. They observed the effect of magnetic field on boundary layer thickness and skin friction at the surface. Boundary layer flow along a flat plate is considered when a magnetic field acts perpendicular to the plate. Recently, Noghrehabadi et al. [24] considered the effect of magnetic field on the boundary layer flow, heat and mass transfer of nanofluids over a stretching cylinder. Ishak et al. [25] studied the effect of a uniform transverse magnetic field on the stagnation point flow over a stretching and vertical sheet. While, Isa et al. [26] studied the effect of magnetic field on mixed convection boundary layer flow over an exponentially shrinking vertical sheet with suction.

The aim of the present paper is to investigate the unsteady MHD boundary layer flow of a Casson fluid development caused by an impulsively stretching surface using numerical approach called spectral quasi-linearization method. Finding an optimal numerical solution to the problem of unsteady boundary layer flow due to stretching sheeting that valid for all time, has been a subject of investigations over time by many researchers. In recent years, there has been an increasing amount of literatures that have adopted Liao's analytic approach in solving unsteady boundary layer flows. However, there are limits to how far analytic approaches can be utilised in nonlinear systems of PDEs involving many equations. Nonlinear systems involving many coupled equations are very difficult to solve analytically. In this work, the spectral quasi-linearization method (SQLM) is apply to solve nonlinear PDEs describing unsteady boundary layer flow of Casson fluid due to an impulsively stretching surface. In the SQLM, the governing nonlinear equations are linearized using the Newton-Raphson based quasi-linearization method (QLM), developed by Bellman and Kalaba [27], and are then integrated using Chebyshev spectral collocation method. Spectral method based quasi-linearisation schemes have also been successfully applied to a range of fluid mechanics based ODE model problems (see [28]-[30]).

In this review, investigation is focus on the unsteady boundary layer flow due to an impulsively stretching surface that was previously discussed by Liao [6] using the homotopy analysis method and recently reported in Ishak [3] and Srinivasa [22] using the Keller-box method. Our purpose is to investigate effects of transverse magnetic field, Casson fluid parameter and the applicability of the new SQLM approach to systems of nonlinear PDE-based unsteady boundary layer flows of varying levels of complexity. Numerical simulations are conducted on the sample problems using SQLM. The method is compared in terms of accuracy, with the reported results in literatures.

The rest of the paper is organized as follows: Section 2 discusses the mathematical formulation of an unsteady MHD boundary-layer flow of Casson fluid caused by an impulsively stretching plate. Section 3 presents the imple- mentation of SQLM on an unsteady MHD boundary layer flow of Casson fluid. Section 4 contains the results and discussion, and the conclusions are given in Section 5.

2. Governing Equations

Following Nadeem et al. [4], Liao [6] and Srinivasa and Eswara [17], an unsteady two-dimensional flow of an incompressible Casson fluid over a stretching surface is examined. The fluid is an electrically conducting fluid in the presence of a fixed applied

magnetic field B_o. A magnetic field B_o of uniform strength is applied transversely to the direction of the flow. Since the fluid pressure is constant throughout the boundary, it is assumed that induced magnetic field is small in comparison to the applied magnetic field; hence it is neglected. It is also assume that the

Rheological equation of Casson fluid, following Mustafa et al. [21], is given as :

$$\tau_{ij} = \left[\mu_c + \left(\frac{P_y}{\sqrt{2\pi}}\right)^{1/n}\right]^n 2e_{ij} \tag{1}$$

where μ_c is plastic dynamic viscosity of the non-Newtonian fluid, P_y is the yield stress of fluid, π is the product of the component of deformation rate with itself, namely, $\pi = e_{ij}e_{ij}$, e_{ij} is the (i, j) th component of the deformation rate. Where n 1 is an arbitrary constant. However, in many application this value is $n \gg 1$. With this in mind and aforementioned assumptions, The boundary-layer equations based on conservation of mass and momentum, governing the unsteady two-dimensional flow on the impulsively stretching surface is:

$$\frac{\partial u}{\partial x} + \frac{\partial v}{\partial y} = 0, \tag{2}$$

$$\frac{\partial u}{\partial t} + u\frac{\partial u}{\partial x} + v\frac{\partial u}{\partial y} = \vartheta\left(1 + \frac{1}{\beta}\right)\frac{\partial^2 u}{\partial y^2} - \sigma\frac{\beta_0^2}{\rho}u. \tag{3}$$

here x and y are the longitudinal and the normal directions respectively. u and v are the velocity components in the x and y-directions respectively, B_o is the magnetic field applied in the y- direction, ρ is the fluid density, ϑ is the kinematic viscosity, σ is the electrical conductivity and β is the Casson fluid parameter. The corresponding boundary conditions are:

$$\begin{aligned} t < 0: &\quad u(x,y,t) = v(x,y,t) = 0, \qquad y = 0 \\ t \geq 0: &\quad u(x,0,t) = ax, \\ &\quad v(x,0,t) = 0, \qquad u(x,\infty,t) = 0 \end{aligned} \tag{4}$$

where constant a is positive number. Now the time scale ξ is choosen such as given above so that the region of the time integration can be finite.

One such transformations is given by Williams and Rhyne [33]. The transformations are expressed as;

$$\xi = 1 - e^{-\tau}, \quad \tau = bt,$$

where b is a positive constant and t is the time variable.

The Williams and Rhyne [33] transformation are used to convert from the infinite (original) time scale $0 \leq \tau \leq 1$ to the finite scale $0 \leq \xi \leq 1$ so that the interval of integration is collapsed from an infinite domain to a finite domain.

The similarity variables given in [22] are utilized and are defined as;

$$\begin{aligned} u = \frac{\partial \psi}{\partial y}, \qquad v = -\frac{\partial \psi}{\partial x}, \\ \psi = \sqrt{b\vartheta\xi}\, x f(\xi,\eta), \qquad \eta = \sqrt{\frac{b}{\vartheta\xi}}\, y. = \end{aligned} \tag{5}$$

Equation (2) is satisfied identically and equation (3) becomes:

$$\begin{aligned} \left(1 + \frac{1}{\beta}\right)f''' + \frac{\eta}{2}(1-\xi)f'' + \xi\left[ff'' - f'^2\right] \\ -\xi M f' = \xi(1-\xi)\frac{\partial f'}{\partial \xi}. \end{aligned} \tag{6}$$

Subject to the boundary condition:

$$f(0,\xi) = 0, \quad f'(0,\xi) = 1, \quad f'(\infty,\xi) = 0 \tag{7}$$

In the above equations, the prime denotes the derivative with respect to η, $(c = \frac{b}{a})$ which indicate that the stretching sheet parameter is a positive constant. The local Hartman number M (Magnetic parameter) and the non-newtonian Casson fluid parameter β are defined as;

$$M = \frac{\sigma B_0^2}{b\rho} \qquad B = \frac{\mu_c\sqrt{2\pi}}{P_y}.$$

In the analysis of boundary layer flow problems, a quantity of physical interest is the skin friction which is given

$$C_f = \frac{\tau_\omega}{\mu_c^b}$$

where

$$\tau_\omega = (\mu_c + \frac{P_y}{\sqrt{2\pi}})$$

Now adopting the expressions in equation 5, the dimensionless form of the skin-friction coefficient is

$$C_f\sqrt{\xi} = (1 + \frac{1}{\beta})\sqrt{Re_x}f''(0,\xi)$$

where Re_x is the local reynold number defined as $\frac{bx^2}{\vartheta}$.

The unsteady case can be divided into two cases:

1. Initial unsteady state flow (t = 0). When τ = 0 corresponding to ξ = 0 and $\beta = \infty$, equation (6) becomes Rayleigh ordinary differential equation viz.,

$$f''' + \frac{\eta}{2}f'' = 0 \tag{8}$$

Subject to the boundary condition:

$$f(0,0) = 0, \quad f'(0,0) = 1, \quad f'(\infty,0) = 0 \tag{9}$$

Equations (8) together with the boundary conditions (9) admit the closed form analytical solution for the initial unsteady state when ξ = 0 given by Srinivasa [22] as:

$$\begin{aligned} f(\eta,0) = \eta erfc\left(\frac{\eta}{2}\right) \\ +(\frac{2}{\sqrt{\pi}})\left[1 - \exp(\frac{-\eta^2}{4})\right] \end{aligned} \tag{10}$$

with

$$erfc(\eta) = (\frac{2}{\sqrt{\pi}}) \int_0^{\eta} e^{-t^2}\, dt \tag{11}$$

defined as the complementary error function

2. Final steady state flow (ξ = 1) When (ξ = 1), corresponding to $\tau = \infty$ and $\beta = \infty$, equation(6) becomes Crane type ordinary differential equation viz.,

$$f''' + ff'' - f'^2 - Mf' = 0 \tag{12}$$

Subject to the boundary condition:

$$f(0,1) = 0, \;\; f'(0,1) = 1, \;\; f'(\infty,1) = 0 \tag{13}$$

The exact solution of (12) is given by

$$f(\eta,1) = \gamma^{-1}[1 - \exp(-\gamma\eta)]$$

where

$$\gamma = (1+M)^{1/2}$$

3. Method of solution

The nonlinear partial differential equation (6) subject to boundary conditions (7) is solved numerically using spectral quasi-linearization method (SQLM). In applying spectral quasi-linearization method to the above governing equation, equation (6) is separate into linear and non -linear part and called them linear operator F and non-linear operator H respectively. This is expressed as :

$$F(f,f',f'',f''') = \left(1+\frac{1}{\beta}\right)f''' + \frac{\eta}{2}(1-\xi)f'' - \xi M f' - \xi(1-\xi)\frac{\partial f'}{\partial \xi}, \tag{14}$$

$$H(f,f',f'',f''') = \xi\left[ff'' - f'^2\right].$$

Then by linearized the non-linear operator H by using the equation

$$H \approx H\left(f_r, f'_r, f''_r, f'''_r\right) + \sum_{k=0}^{3} \phi_{k,r} f_{r+1}^{(k)} - \sum_{k=0}^{3} \phi_{k,r} f_r^{(k)}. \tag{15}$$

The coefficients $\phi_{k,r}$ in the above equation are given as

$$\phi_{0,r} = \frac{\partial H}{\partial f}\left[f_r, f'_r, f''_r, f'''_r\right] = \xi f''_r, \qquad \phi_{1,r} = \frac{\partial H}{\partial f'}\left[f_r, f'_r, f''_r, f'''_r\right] = -2\xi f'_r, \tag{16}$$

$$\phi_{2,r} = \frac{\partial H}{\partial f''}\left[f_r, f'_r, f''_r, f'''_r\right] = \xi f_r, \qquad \phi_{3,r} = \frac{\partial H}{\partial f'''}\left[f_r, f'_r, f''_r, f'''_r\right] = 0. \tag{17}$$

And

$$R_r = \sum_{k=0}^{3} \phi_{k,r} f_r^{(k)} - \sum_{k=0}^{3} \phi_{k,r} f_r^{(k)} - H(f_r, f'_r, f''_r, f'''_r) = \xi f_r f''_r - \xi (f'_r)^2 \tag{18}$$

Such that the linearized form of the governing equation (6) is

$$F[f_{r+1}, f'_{r+1}, f''_{r+1}, f'''_{r+1}] + \sum_{k=0}^{n} \phi_{k,r} f_{r+1}^{(k)} - f_{r+1} = R_r[f_r, f'_r, f''_r, f'''_r] \tag{19}$$

simplified further as

$$a_{0,r}(\eta,\xi)f'''_{r+1} + a_{1,r}(\eta,\xi)f''_{r+1} + a_{2,r}(\eta,\xi)f'_{r+1} + a_{3,r}(\eta,\xi)f_{r+1} - \xi(1-\xi)\frac{\partial f'_{r+1}}{\partial \xi} = a_{4,r}(\eta,\xi). \tag{20}$$

Subject to

$$f_{r+1}(0,\xi) = f'_{r+1}(\infty,\xi) = 0, \;\; f'_{r+1}(0,\xi) = 1 \tag{21}$$

where

$$a_{0,r}(\eta,\xi) = \left(1+\frac{1}{\beta}\right), \quad a_{1,r}(\eta,\xi) = \frac{\eta}{2}(1-\xi) + \xi f_r,$$
$$a_{2,r}(\eta,\xi) = -2\xi f'_r - \xi M, \quad a_{3,r}(\eta,\xi) = \xi f''_r,$$
$$a_{4,r}(\eta,\xi) = \xi f_r f''_r - \xi (f'_r)^2.$$

The initial approximation for solving (20)-(21) is obtained as the solutions at ξ = 0. Hence $f_0(\eta, \xi)$ as

$$f_0(\eta,0) = \eta erfc\left(\frac{\eta}{2}\right) + (\frac{2}{\sqrt{\pi}})\left[1 - \exp(-\frac{\eta^2}{4})\right] \tag{22}$$

The solution for the linearized PDE (20) is obtained by approximating the exact solution of $f(\eta, \xi)$ by the initial approximations given in (22) and a Lagrange form of polynomial $F(\eta,)$ which interpolates $f(\eta, \xi)$ at the selected points (called collocation points):

$$0 = \xi_0 < \xi_1 < \xi_2 < \cdots < \xi_{N_\xi} = 1$$

Therefore the approximation for $f(\eta, \xi)$ has the form

$$f(\eta,\xi) \approx \sum_{l=0}^{N_\xi} F(\eta,\xi_j)L_j(\xi) = \sum_{l=0}^{N_\xi} F_j(\eta)L_j(\xi), \tag{23}$$

Which interpolates $f(\eta,\xi)$ at the collocation points defined above. It is remark that, for ease of notation, the subscripts *r+1* is dropped. The function $L_j(\xi)$ is the well-known characteristic Lagrange cardinal polynomials:

$$L_j(\xi) = \prod_{\substack{j=0 \\ j\neq k}}^{M} \frac{\xi - \xi_k}{\xi_j - \xi_k}, \;\; L_j(\xi_k) = \delta_{jk} = \begin{cases} 0 & if\ j \neq k \\ 1 & if\ j = k \end{cases} \tag{24}$$

The equations for the solution of $F_j(\eta)$ are obtained by substituting (23) in (20) and compelling the equation to be satisfied exactly at the points ξ_i, i=0,1,2,...,N_ξ. This process is called collocation. To enable the derivatives of the Lagrange polynomial with respect to ξ to be computable analytically, it is convenient to transform the interval $\xi\epsilon$[0, 1] to $\zeta\epsilon$[−1, 1] then choose Chebyshev-Gauss-Lobatto points

$$\zeta_i = \cos(\frac{i\pi}{N_\xi}),$$

as the collocation points. After using linear transformation to transform ξ to the new variable ζ, the derivative of f with respect to ξ at the collocation points ζ_j is computed as

$$\left.\frac{\partial f'}{\partial \xi}\right|(\xi = \xi_i) = 2\sum_{j=0}^{N_\xi} F_j'(\eta)\frac{dL_j}{d\zeta}(\zeta_i) = 2\sum_{j=0}^{N_\xi} F_j'(\eta)d_{i,j},$$

$$i = 0,1,2,3,\cdots,N_\xi \tag{25}$$

where $d_{i,j} = \frac{dL_j}{d\xi}(\xi_i)$, $i = 0,1,2,3,\cdots,N_\xi$ are entries of the standard Chebyshev differentiation matrix. Applying the collocation at ξ_i in (20) gives

$$a_{0,r}^{(i)} f_{r+1}'''(\eta) + a_{1,r}^{(i)} f_{r+1}''(\eta) + a_{2,r}^{(i)} f_{r+1}'(\eta) + a_{3,r}^{(i)} f_{r+1}(\eta)$$

$$-2\xi_i(1-\xi_i)\sum_{j=0}^{N_\xi} F_j'(\eta)d_{i,j} = a_{4,r}^{(i)}. \tag{26}$$

where $a_{k,r}^{(i)} = a_{k,r}(\eta,\xi), k = 0,1,2,3,4$. Since the solution at ξ=0 and ξ=ξN_ξ is known, Then equation (29) is only evaluate for i=0,1,2,...,N_ξ −1. The resulting systems becomes

$$a_{0,r}^{(i)} f_{r+1}'''(\eta) + a_{1,r}^{(i)} f_{r+1}''(\eta) + a_{2,r}^{(i)} f_{r+1}'(\eta) + a_{3,r}^{(i)} f_{r+1}(\eta)$$

$$-2\xi_i(1-\xi_i)\sum_{j=0}^{N_\xi} F_j'(\eta)d_{i,j} \tag{27}$$

$$= a_{4,r}^{(i)} + 2\xi_i(1-\xi_i)d_{i,N_\xi}F_{r+1,N_\xi}'(\eta).$$

It is worth note that for each ξ_i, equation (27) forms a linear ordinary equation with variable coefficients. To solve equation (27) Chebyshev spectral collocation is apply independently in the η direction by choosing N_η+1 Chebyshev- Gauss-Lobatto points $0=\eta_0<\eta_1<\eta_2<\eta_0<\ldots<\eta N_\eta=\eta_e$, where η_e is a finite value that is chosen to be suffiently large to approximate the conditions at ∞. Again, before implementing the collocation, the interval $\eta\epsilon[0,\eta_e]$ is transformed into $\iota\epsilon[-1,1]$ using a linear transformation. Thus, the collocation points are chosen as

$$\iota_j = \cos(\frac{j\pi}{N_\eta}),$$

The derivatives with respect to η are defined is terms of the Chebyshev differentiation matrix as

$$\left.\frac{d^p F_{r+1,i}}{d\eta^p}\right|(\eta = \eta_e) = \left(\frac{2}{\eta_e}\right)^p \sum_{k=0}^{N_\eta} D_{j,k}^p F_{r+1,i}(\iota_k) = D^p F_{r+1,i} \tag{28}$$

where p is the order of the derivative, $D = \left(\frac{2}{\eta_e}\right)[D_{j,k}](j,k = 0,1,2,\cdots,N_\eta)$ with $[D_{j,k}]$ being an $(N_\eta+1)\times((N_\eta+1))$.

Chebyshev derivative matrix, and the vector $F_{r+1,i}$ is defined as $F_{r+1,i}=[F_{r+1,i}(\iota_0), F_{r+1,i}(\iota_1), F_{r+1,i}(\iota_2,..., F_{r+1,i}(\iota_N))]^T$

By substituting equation (28) into (27), yields:

$$A^{(i)}F_{r+1,i} - 2\xi_i(1-\xi_i)\sum_{j=0}^{N_\xi-1} D\,F_{r+1,j} = R^{(i)}. \tag{29}$$

where

$$A^{(i)} = a_{0,r}^{(i)}D^3 + a_{1,r}^{(i)}D^2 + a_{2,r}^{(i)}D + a_{3,r}^{(i)},$$

$$R^{(i)} = a_{3,r}^{(i)} + 2\xi_i(1-\xi_i)\sum_{j=0}^{N_\xi-1} d_{i,N_\xi}D\,F_{r+1,N_\xi}.$$

where $a_{k,r}^{(i)}(k = 0,1,2,3)$ is a diagonal matrix with the vector $\left[a_{k,r}^{(i)}(\iota_0), a_{k,r}^{(i)}(\iota_1), \ldots, a_{k,r}^{(i)}(\iota_{N_x})\right]^T$ placed on the main diagonal. After substituting the boundary conditions, for each i=0,1,...,N_ξ-1, equation (29) can be written in matrix form as

$$\begin{bmatrix} A_{0,0} & A_{0,1} & \ldots & A_{0,N_\xi-1} \\ A_{1,0} & A_{1,1} & \ldots & A_{1,N_\xi-1} \\ \vdots & \vdots & \ddots & \vdots \\ A_{N_\xi-1,0} & A_{N_\xi-1,1} & \cdots & A_{N_\xi-1,N_\xi-1} \end{bmatrix}\begin{bmatrix} F_{r+1,0} \\ F_{r+1,1} \\ \vdots \\ F_{r+1,N_\xi-1} \end{bmatrix} = \begin{bmatrix} R_1^0 \\ R_1^1 \\ \vdots \\ R_1^{N_\xi-1} \end{bmatrix} \tag{30}$$

where

$$A_{i,i} = A^{(i)} - 2\xi_i(1-\xi_i)d_{i,i}D, \qquad i = 0,1,2,,\cdots,N_\xi - 1$$

$$A_{i,i} = -2\xi_i(1-\xi_i)d_{i,j}D, \quad where\ i \neq j$$

Hence, starting from the initial approximations $f_0(\eta,\xi)$; given by equations (10), equations (29) can be solved iteratively to give approximate solutions for $f_{r+1}(\eta, \xi)$ r=0, 1, 2,... until a solution that converges to a given accuracy is obtained.

Table 1. Computed values of wall shear stress $f''(\xi, 0)$ using QSLM as compared with other results in literatures for different values of ξ, when $\beta = \infty$ and $M = 0.0$

ξ	Ref. [6]	Ref. [31]	Ref. [32]	Ref. [22]	Present result
0.1	-0.6106105684	-0.6150155043	-0.6106968740	-0.6106120	-0.6104674607
0.3	-0.7015602589	-0.7116696045	-0.7014912575	-0.7115610	-0.7012666313
0.5	-0.7904118776	-0.8018198801	-0.7900472367	-0.8004117	-0.7898281748
0.7	-0.8773153545	-0.8856581275	-0.8764799121	-0.8873160	-0.8762663192
0.8	-0.9200563754	-0.9252701770	-0.9198114759	-0.9200550	-0.9187007163
0.9	-0.9623399700	-0.9633761429	-0.9607448540	-0.9623398	-0.9605377533
1.0	-	-	-1.0000000000	-1.0000000	-0.9951954343

Table 2. Computed values of wall shear stress $f''(\xi,0)$ for various values of Magnetic parameter M when $\beta = 100, \xi = 0.5$

M	$f''(\xi, 0)$
0.0	-0.7878602743
0.5	-0.9121941670
0.7	-0.9591901558
1.0	-1.0270440776

Table 3. Computed values of wall shear stress $f''(\xi,0)$ for various values of Casson fluid parameter β when $M = 0.5, \xi = 0.5$

β	$f''(\xi, 0)$
1.0	-0.7465920225
10	-0.8924220729
100	-0.9121941670
∞	-0.9144728990

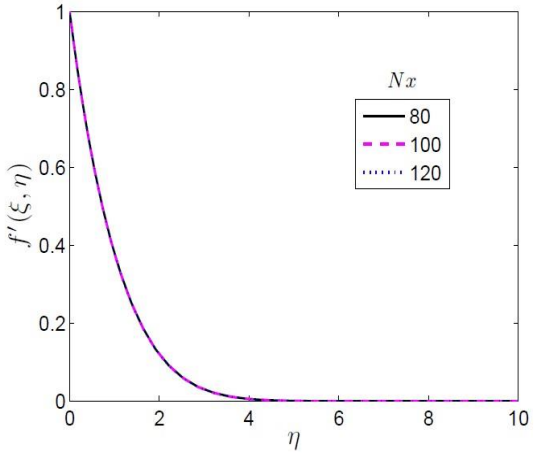

Figure 1. Velocity profile of the Casson fluid at different collocation point along η domain to check grid independent test.

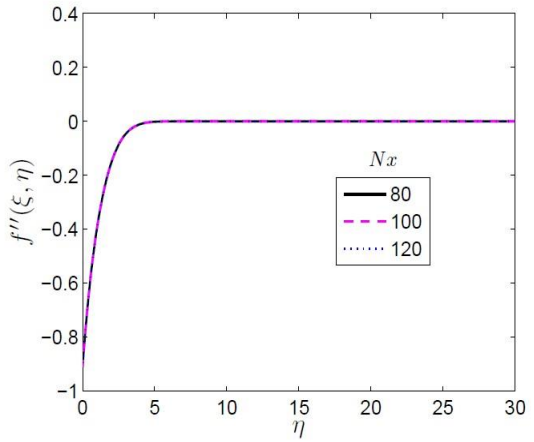

Figure 2. Skin-friction coefficient profile of the Casson fluid at different collocation point along η domain to check grid independent test.

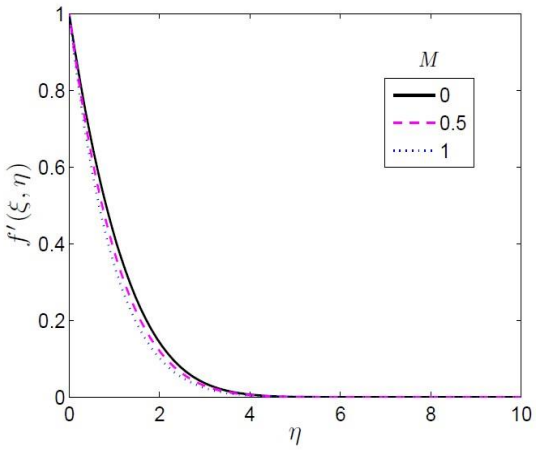

Figure 3. Effect of magnetic parameter (M) on velocity profile of the Casson fluid.

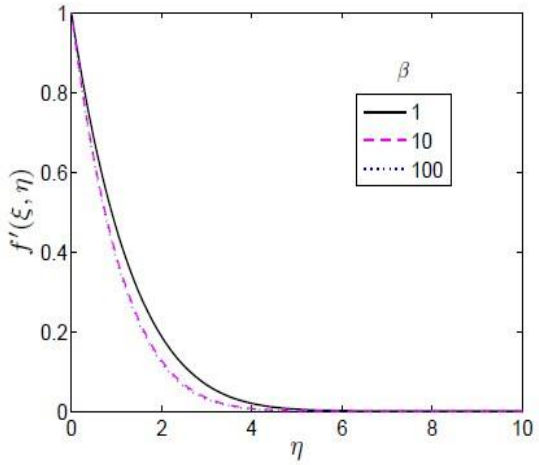

Figure 4. Effect of Casson fluid parameter (β) on velocity profile of the fluid.

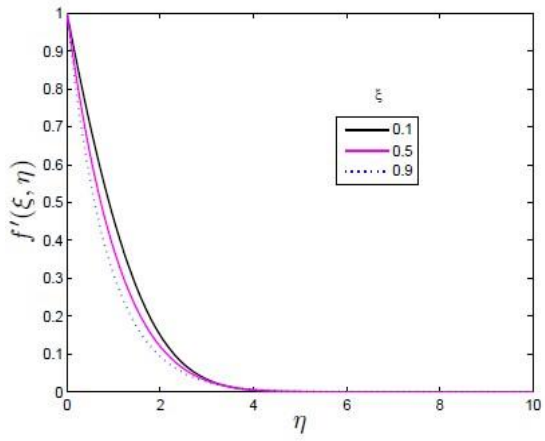

Figure 5. Velocity profile of the Casson fluid for various values of ξ

4. Results and Discussion

In this section, the numerical results obtained using spectral quasi-linearization method (SQRM) on the governing nonlinear partial differential equation (6) is presented. Numerical computation were carried out using the proposed method as discussed in the previous sections for the velocity and the local skin friction for different values of the significant physical parameters in this study. Results are displayed in tabular and graphical formats. The SQRM was used to generate results from the initial approximate at ξ=0 up to results close to the steady state values at ξ=1. The accuracy of the computed SQRM results was validated against numerical results obtained using the Keller-box method as reported in literatures.The results presented in this work were generated using L=30, which was found to give accurate results through numerical experimentation. In computing the numerical results presented in this paper, unless otherwise stated, the following values of physical parameters were used: M= 0.5, β=10, ξ=0.5 and Nt =50. Grid independence tests as illustrated in Figures 1 and 2 revealed that N_x = 120 and N_t = 50 collocation points in the η and ξ domain, respectively, were sufficient to give accurate and consistent results. A further increase in the number of collocation points did not result in a change in the computed results. Furthermore, the minimum number of iterations required to give results that are consistent to within a tolerance level of 10^{-7} were used. In all the results presented below, it was found that 50 iterations were sufficient to give consistent results. The value of η_∞ was set to be 10. All graphs and tables therefore corresponds to these values except otherwise indicated. The values of all other physical parameters governing the fluid flow are chosen based on values earlier used in literatures.

In order to test the method of solution,the special case of the problem is solved and compared with Liao [6], Srinivasa [22], Awang [31] and Fadzilah [32] in Table 1. Table 1 is drawn for a special case when pertinent parameters M=ξ=0 and β=∞ . The available results obtained in literatures above and SQRM are compared and are in very good agreement. The comparison shows that the present results obtained using SQLM has an excellent agreement with the solution obtained using other method of solution such as implicit finite difference scheme called Keller-box method and homotopy analysis method (HAM).

Table 2 gives account on the effect of the Magnetic parameter M, on local wall shear stress of the flow. From the Table 2, It is noticed that an increase in the values of magnetic parameter M results in narrowing of horizontal velocity of the fluid. The transverse contraction of the velocity boundary layer is due to the applied magnetic field which invokes the Lorentz force producing noticeable opposition to the fluid flow. Hence, the magnetic parameter M influences the control of surface shear stress.Further, it is found that absolute value of $f''(0, \xi)$ increases with the increase of magnetic field M. This is because when M increases, the Lorentz force produces more resistance to the transport phenomena which leads to the deceleration of the flow, enhancing the surface shear stress. These results are in good agreement with those obtained by Srinivasa and Eswara [22].

Similarly Table 3 gives the skin friction coefficient for selected Casson fluid parameter β values. Here It is observed that as the Casson fluid parameter increase, the absolute values of skin friction coefficient increases.

In Fig. 3, the effect of increasing the magnetic field strength on the momentum boundary layer thickness is illustrated. It is established fact that the magnetic field presents a damping effect on the velocity field by creating drag force that opposes the fluid motion, causing the velocity to decease.That is the boundary layer thickens and the magnitude of the velocity decreases with an increase in Hartmann number,M. This clearly indicates that the transverse magnetic field opposes the transport phenomena. This is because the variation of M leads to the variation of Lorentz force due to the magnetic field, and the Lorentz force produces more resistance to the transport phenomena. Therefore, the momentum boundary layer thickness becomes larger, and the separation of the boundary layer occurs earlier.

Figure 4 shows the graphical influence of fluid Casson parameter β on the velocity profile of the flow. It shows that the magnitude of velocity and boundary layer thickness decreases with an increase in Casson fluid parameter, β. It is noticed that when the fluid parameter approaches infinity, the problem in the given case reduces to a Newtonian case.

Figure 5 exhibits velocity profiles for different values of ξ. It is obvious from this figure that increase in ξ results in the reduction of momentum boundary layer thickness and thereby enhancing the velocity gradient at the surface. Further, the velocity profiles decrease monotonically with the distance from the surface and finally become zero for away from it, satisfying the boundary conditions asymptotically, and thus supporting the numerical results obtained.

5. Conclusions

The study investigated the application of the spectral quasi-linearization technique coupled with the Chebyshev pseudo-spectral collocation method to obtain a numerical solution of unsteady MHD boundary layer flow of Casson fluid due to an impulsively stretching surface. Approximate numerical results were generated using spectral quasi-linearization for the solution of the skin friction coefficient as well as velocity profile of the fluid at different flow parameter values. The accuracy of the

SQLM was demonstrated by comparing with results generated using the implicit finite difference method (keller box) and homotopy analysis method (HAM) and a good agreement was achieved between the two set of results up to a fixed level of accuracy. Other parameters which appear to have a marginal influence on the velocity distribution also have strong influence on the surface shear stress.

The study showed that the SQLM can be used as an alternative method to obtain numerical solutions of partial differential equations (PDEs). The SQLM approach presented in this study also adds to a growing body of literature on numerical methods for solving complex nonlinear fluid flow problems in fluid mechanics. The results reveal that:

- An increase in the Casson fluid parameter β of Casson fluid corresponds to an increase in the velocity profiles.
- The magnetic field exerts significant influence on skin friction coefficient and reduces the momentum boundary layer thickness

Conflicts of Interest

The author declares that there is no conflict of interest regarding the publication of this manuscript. In addition, the authors have entirely observed the ethical issues, including plagiarism, informed consent, misconduct, data fabrication and/or falsification, double publication and/or submission, and redundancy.

References

[1] Bird, R.B., Stewart, W.E. and Lightfoot, E.N, 2007. Transport Phenomena (Revised Second Edition ed.) John Wiley and Sons. ISBN 978-0-470-11539-8.

[2] Chiam, T.C., 1993. Magnetohydrodynamic boundary layer flow due to a continuously moving flat plate. *Computers & Mathematics with Applications*, *26*(4), pp.1-7.

[3] Ishak, A., Nazar, R. and Pop, I., 2009. Heat transfer over an unsteady stretching permeable surface with prescribed wall temperature. *Nonlinear Analysis: Real World Applications*, *10*(5), pp.2909-2913.

[4] Nadeem, S., Haq, R.U. and Lee, C., 2012. MHD flow of a Casson fluid over an exponentially shrinking sheet. *Scientia Iranica*, *19*(6), pp.1550-1553.

[5] Sakiadis, B.C., 1961. Boundary-layer behavior on continuous solid surfaces: II. The boundary layer on a continuous flat surface. *AiChE journal*, *7*(2), pp.221-225.

[6] Liao, S., 2006. An analytic solution of unsteady boundary-layer flows caused by an impulsively stretching plate. *Communications in Nonlinear Science and Numerical Simulation*, *11*(3), pp.326-339.

[7] Nazar, R., Ishak, A. and Pop, I., 2008. Unsteady boundary layer flow over a stretching sheet in a micropolar fluid. *International Journal of Mathematical, Physical and Engineering Sciences*, *2*(3), pp.161-165.

[8] Takhar, H.S., Chamkha, A.J. and Nath, G., 2001. Unsteady three-dimensional MHD-boundary-layer flow due to the impulsive motion of a stretching surface. *Acta Mechanica*, *146*(1-2), pp.59-71.

[9] Hayat, T., Shehzad, S.A. and Alsaedi, A., 2012. Soret and Dufour effects on magnetohydrodynamic (MHD) flow of Casson fluid. *Applied Mathematics and Mechanics*, *33*, pp.1301-1312.

[10] Prasad, K.V. and Vajravelu, K., 2009. Heat transfer in the MHD flow of a power law fluid over a non-isothermal stretching sheet. *International Journal of Heat and Mass Transfer*, *52*(21-22), pp.4956-4965.

[11] Abel, M.S., Siddheshwar, P.G. and Mahesha, N., 2009. Effects of thermal buoyancy and variable thermal conductivity on the MHD flow and heat transfer in a power-law fluid past a vertical stretching sheet in the presence of a non-uniform heat source. *International journal of non-linear mechanics*, *44*(1), pp.1-12.

[12] Bhattacharyya, K. and Pop, I., 2011. MHD boundary layer flow due to an exponentially shrinking sheet. *Magnetohydrodynamics*, *47*(4), pp.337-344.

[13] Bhattacharyya, K., 2013. Boundary layer stagnation-point flow of Casson fluid and heat transfer towards a shrinking/stretching sheet. *Frontiers in Heat and Mass Transfer (FHMT)*, *4*(2).

[14] Astarita, G. and Marrucci, G., 1974. Principles of non-Newtonian fluid mechanics.

[15] Shenoy, A.V. and Mashelkar, R.A., 1982. Thermal convection in non-Newtonian fluids. In *Advances in heat transfer* (Vol. 15, pp. 143-225). Elsevier.

[16] Crochet, M.J. and Walters, K., 1983. Numerical methods in non-Newtonian fluid mechanics. *Annual Review of Fluid Mechanics*, *15*(1), pp.241-260.

[17] Casson, N., 1959. Flow equation for pigment-oil suspensions of the printing ink-type. *Rheology of disperse systems*, pp.84-104.

[18] Subba Rao, A., Ramachandra Prasad, V., Bhaskar Reddy, N. and Anwar Bég, O., 2015. Heat transfer in a Casson rheological fluid from a semi-infinite vertical plate with partial slip. *Heat Transfer—Asian Research*, *44*(3), pp.272-291.

[19] Bird, R.B., Dai, G.C. and Yarusso, B.J., 1983. The rheology and flow of viscoplastic materials. *Reviews in chemical engineering*, *1*(1), pp.1-70.

[20] Mukhopadhyay, S., 2013. Casson fluid flow and heat transfer over a nonlinearly stretching surface. *Chinese Physics B*, *22*(7), p.074701.

[21] Mustafa, M., Hayat, T., Pop, I. and Aziz, A., 2011. Unsteady boundary layer flow of a Casson fluid due to an impulsively started

moving flat plate. *Heat Transfer—Asian Research*, *40*(6), pp.563-576.

[22] Srinivasa, A.H. and Eswara, A.T., 2014. Unsteady MHD Laminar Boundary Layer Flow and Heat Transfer due to an Impulsively Stretching Surface. *International Journal of Modern Sciences and Engineering Technology (IJMSET). V1*, (7), pp.32-40.

[23] Shrivastava, U.N. and Usha, S., 1987. Magneto-fluid dynamic boundary layer on a moving continuous flat surface. *Indian J. pure appl. Math*, *18*, pp.741-751.

[24] A. Noghrehabadi, M. Ghalambaz, E. Izadpanahi and R. Pourrajab. Effect of Magnetic Filed on the Boundary Layer Flow, Heat and Mass Transfer of Nanofluids over a Stretching Cylinder. Journal of Heat and Mass Transfer Research, 2014;1: 9-16.

[25] Ishak, A., Nazar, R. and Pop, I., 2008. Hydromagnetic flow and heat transfer adjacent to a stretching vertical sheet. *Heat and Mass Transfer*, *44*(8), pp.921-927.

[26] Isa, S.S.P.M., Arifin, N.M., Nazar, R., Bachok, N., Ali, F.M. and Pop, I., 2014. Effect of magnetic field on mixed convection boundary layer flow over an exponentially shrinking vertical sheet with suction. *International Journal of Mechanical, Aerospace, Industrial and Mechatronics Engineering*, *8*, p.1519.

[27] Bellman, R.E., 1965. *Quasilinearization and nonlinear boundary-value problems* (Vol. 3). American Elsevier Publishing Company.

[28] Motsa, S.S., Hayat, T. and Aldossary, O.M., 2012. MHD flow of upper-convected Maxwell fluid over porous stretching sheet using successive Taylor series linearization method. *Applied Mathematics and Mechanics*, *33*, pp.975-990.

[29] Motsa, S.S. and Shateyi, S., 2012. Successive linearization analysis of the effects of partial slip, thermal diffusion, and diffusion-thermo on steady MHD convective flow due to a rotating disk. *Mathematical Problems in Engineering*, *2012*.

[30] Awad, F.G., Sibanda, P., Motsa, S.S. and Makinde, O.D., 2011. Convection from an inverted cone in a porous medium with cross-diffusion effects. *Computers & Mathematics with Applications*, *61*(5), pp.1431-1441.

[31] Kechil, S.A. and Hashim, I., 2007. Series solution for unsteady boundary-layer flows due to impulsively stretching plate. *Chinese Physics Letters*, *24*(1), p.139.

[32] Md, A.F., Roslinda, N.A.Z.A.R. and Md, A.N., 2010. Numerical solutions of unsteady boundary layer flow due to an impulsively stretching surface. *Journal of Applied Computer Science & Mathematics*, *4*(2), pp.25-30.

[33] Williams, III, J.C. and Rhyne, T.B., 1980. Boundary layer development on a wedge impulsively set into motion. *SIAM Journal on Applied Mathematics*, *38*(2), pp.215-224.